Transmission and magnetoacoustic efficiencies in ferromagnetic conducting films

C. Vittoria, M. Rubinstein, and P. Lubitz
Naval Research Laboratory, Washington, D.C. 20375
(Received 18 June 1975)

We have formulated a unified theory for calculations of magnetoacoustic efficiencies and ferromagnetic transmission resonance. As specific examples, we have calculated the magnetoacoustic efficiency in thick films of Ni and Tb-Fe; we have also calculated transmission efficiencies for Ni-Fe thick films.

I. INTRODUCTION

The transmission and the magnetoacoustic conversion of an electromagnetic (em) wave in passing through a conducting ferromagnetic film is of practical interest for microwave device applications. Although the problems of transmission of an em wave through a ferromagnetic metal film and of the conversion of this wave into an acoustic wave have been previously presented separately in the literature, we will present a unified treatment of these cases based on a single phenomenological theory.[1] In a previous paper,[1] a general dispersion law was obtained for a magnetoelastic, ferromagnetic, and conductive medium. We now extend the previous calculations to evaluate the transmission and magnetoacoustic conversion efficiencies in a unified treatment by applying boundary conditions appropriate to specific problems.

The transmission of an em wave through a ferromagnetic metal film was first treated theoretically by Kaganov[2] and experimentally by Heinrich and Meshcheryakov.[3] Transmission resonance in metal films occurs at fields well below ferromagnetic resonance. In analogy with other oscillators, the real part of the susceptibility χ is negative for fields below (corresponding to frequencies above) ferromagnetic resonance and positive above resonance. Thus, the permeability μ of the material can approach zero for fields below resonance, since μ is defined as

$$\mu = 1 + 4\pi\chi . \tag{1}$$

The field for which $\mu \to 0$ has been defined by Kittel[4] as the *antiresonance* field, in contrast to the ferromagnetic resonance field at which $\mathrm{Im}(\mu)$ is maximum. In magnetic materials, however, μ is not exactly equal to zero, since μ is complex.

Thus, as noted by Kaganov,[2] the skin depth δ in a ferromagnetic *metal* increases near antiresonance, since $\delta \propto 1/\sqrt{\mu}$. This allows an em wave to be transmitted through even a relatively thick metal ferromagnetic film near antiresonance. This transmission resonance was in fact demonstrated by Heinrich and Meshcheryakov.[3] The required fields for antiresonance or transmission resonance can be calculated from Eq. (1), putting $\mu = 0$, as demonstrated by Kittel.[4] However, one further requirement, which was omitted in Ref. 4, is that χ must be defined as the *normal-mode* susceptibility. For example, for the static magnetic field perpendicular to the film, the normal modes are circularly polarized. χ would then be defined as the ratio of m/h, where these quantities are the circularly polarized wave amplitudes. If, however, a χ is arbitrarily defined (as in Ref. 4) as the ratio of two linearly polarized quantities, as m_α/h_α, an incorrect field dependence is predicted for the antiresonance. In order to avoid explicitly calculating χ for each angle of the static field $\vec{H}$, it is simpler to assume that one can write the equation of motion for *all* angles of $\vec{H}$ as (neglecting damping for the moment)

$$\dot{M}/\gamma = \vec{M} \times \vec{H} , \tag{2}$$

where $H = \vec{H}_0 + \vec{h}$. $\vec{H}_0$ is the effective static internal field and takes into account the static demagnetizing field. The rf field $\vec{h}$ is the field derived from the antiresonance condition [(Eq. (1)]

$$\vec{h} = -4\pi\vec{m}.$$

It follows then that the antiresonance condition for *all* angles of $\vec{H}_0$ with respect to the film plane is

$$\omega/\gamma = B_0 = H_0 + 4\pi M_0 . \tag{3}$$

We note for the in-plane case

$$\omega/\gamma = H_a + 4\pi M_0 , \tag{4}$$

and for the perpendicular case

$$\omega/\gamma = H_a , \tag{5}$$

where H_a is the external applied field. Maximum transmission in metals occurs for fields slightly shifted from the above expressions. The shift will be calculated later in this paper. A major result of transmission resonance experiments[3] is that the transmission linewidth is directly related to the magnetic damping, while the ferromagnetic resonance (FMR) linewidth in metals is a combination of the intrinsic and exchange-conductivity[5] contri-

butions. In a transmission resonance experiment exchange-conductivity effects are negligible, since the rf fields near antiresonance are characterized by very small spatial variations, especially in comparison with the situation at the ferromagnetic resonance. Thus, one can measure the intrinsic linewidth contribution from the transmission resonance experiment as was done by Heinrich and Meshcheryakov.[3] Of course, the conductivity still plays a crucial role in determining the transmission linewidth and intensity.

Following the work of Kittel,[4] Kaganov,[2] and Heinrich and Meshcheryakov,[3] theoretical and experimental work has been directed at estimating and measuring the effect of conductivity and exchange on the transmission resonance line shape.[6,7] Calculations of the transmission resonance line shapes including exchange and conductivity were done by Phillips[6] and Horan *et al.* only for the case where H_a is perpendicular to the film. In a 10-μm film Phillips[6] observed that transmission maxima occur at two fields for H_a normal to the plate. This was interpreted[6] as the effect of a standing-spin-wave mode on transmission.

We have included the effects of exchange, conductivity, and spin boundary conditions in our calculation of the transmission resonance line shape as a function of the angle α and film thickness. We find for 10-μm films that the effect of standing spin waves is to give rise to a number of transmission resonance peaks and not just *two*[6] peaks. For thick films (~100 μm) only one transmission resonance peak for all angles of H_a is calculated, in agreement with recent experimental findings of Heinrich and Cochran.[8-10] As one would expect, spin boundary conditions become important for film thickness less than the skin depth.

These and previous calculations are normally carried out numerically on a computer. However, for thick films we derive an approximate analytical expression for the transmission resonance field and linewidth.

There are essentially two schemes[11] by which a coherent acoustic wave can be generated in a ferromagnetic film. The first method is to excite the film to ferromagnetic resonance. The magnetoacoustic coupling of the material induces a lattice motion whose amplitude depends on the rf magnetic moment amplitude at resonance and, consequently, on the conductivity. The acoustic-wave amplitude is position dependent, since the rf fields attenuate in the metal film. In order to minimize conductivity losses, the film thickness was chosen[12] to be less than the skin depth. Furthermore, the acoustic power at the rod (where the film is attached) can[12] be optimized by choosing the film thickness to be a half-wavelength of the phonon wave. For this case conductivity effects can be small. In the scheme of Kobayashi *et al.*[12] the acoustic impedance of the rod is chosen to be mismatched to the acoustic impedance of the film so that only part of the acoustic-standing-wave power in the film is launched into the rod. We extended calculations of this first method to consider the case of relatively thick films in which conductivity effects are important, and determine the thickness for which the transducer ceases to be of practical interest. For this calculation we consider a Ni film as an example.

The second method by which phonons can be generated is to bias the magnetic field to magnetic and acoustic resonance simultaneously (crossover region). This requires that the operating frequency coincide with the crossover region, where the spin-wave and acoustic-wave vectors are degenerate. At the crossover region the volume spin-wave branch intersects the two transverse-acoustic branches. The spin-wave branch couples or admixes with one of the transverse-acoustic branches which is polarized in the same sense (see Ref. 1). The magnetoacoustic conversion depends on the magnetostriction constant, the acoustic and the spin-wave damping. In addition, at high frequencies one would expect conductive losses to be important in reducing the over-all transducer efficiency.

A priori it is not clear which of the two schemes should give rise to a higher magnetoacoustic transducer efficiency. Therefore, we have considered both schemes of field biasing in our calculation of transducer efficiencies in films of Ni and in Tb-Fe, where the magnetostriction constant may be large. The calculations will be compared with the magnetoacoustic efficiency measurements of Bömmel and Dransfeld[13] in Ni films and of Donoho *et al.*[14] in Tb-Fe films.

II. MAGNETOACOUSTIC AND ELECTROMAGNETIC EFFICIENCIES

We consider the problem of reflection, transmission, and magnetoacoustic conversion of a plane em wave incident on a magnetic film as in Fig. 1. The quantities of interest are the ratios of (a) the acoustic-wave power and (b) the transmitted em power in medium 3 to the incident em power. The film is characterized by a spontaneous saturation magnetization M_0, exchange stiffness constant A, electrical conductivity σ, magnetic gyromagnetic ratio γ, Landau-Lifshitz damping parameter λ, magnetoacoustic constants B_1 and B_2, magnetic cubic anisotropy constants K_1 and K_2, elastic displacement constants C_{11}, C_{12}, and C_{44}, and elastic relaxation time τ. The film is assumed to be a

{100} plane. The magnetic field direction may be arbitrarily chosen with respect to the film surface. Medium 3 is characterized by an acoustic-wave impedance Z_A. The geometrical configuration and the parameters characterizing media 2 and 3 are of sufficient generality that many configurations can be evaluated. However, we will restrict our calculations to situations where comparison with experiments[13,14] can be made.

The procedure for the calculation of the efficiencies is straightforward:

(i) For a given frequency and magnetic field there are seven[1] allowable propagation constants k_n^2 in a magnetoelastic conductive media. The functional relation between frequency and each k_n or branch for a fixed bias field is given in Ref. 1. Four of the branches are predominantly magnetic and the other three are essentially elastic branches. However, it is important to point out that magnetic attenuation is greatest at FMR, whereas the elastic losses are greatest at the crossover region (for frequency and wave number independent λ and τ).

(ii) For each k_n there corresponds an internal-field solution of the form $h_n e^{-jk_n y}$, where k_n is complex. Since the film thickness d is finite, we must allow for internal reflections, so that for given k_n the internal-field solution is of the form

$$h_n^+ e^{-jk_n d} + h_n^- e^{jk_n d},$$

where $h_n^\pm$ denotes the field amplitude of the wave traveling in the $\pm y$ direction. The amplitude and phase of $h_n^\pm$ are of course determined by the boundary conditions. The internal fields must add up so that both the electric and magnetic rf fields are continuous at each surface. Besides the electromagnetic boundary requirements, we require a boundary condition on the rf magnetic moment $\vec{m}$ and the lattice displacement $\vec{u}$ at the two surfaces.

(iii) The boundary condition on $\vec{m}$ at the surface for a magnetoelastic medium is given as[15]

$$A\frac{\partial m}{\partial y} + K_s m + \frac{B_2}{M_0} u = 0, \quad y = d$$

$$A\frac{\partial m}{\partial y} - K_s m + \frac{B_2}{M_0} u = 0, \quad y = 0$$

where both m and u are circularly polarized and the form of the uniaxial surface energy is taken to be $E_s = K_s \alpha_2^2$, where $\alpha_2 = \sin\theta \sin\phi$. These surface pinning conditions apply *only* for $\vec{H}_a$ normal to the film surface. Pinning boundary conditions for arbitrary angle will be considered in the transmission resonance case.

Let us now estimate the coupling term and compare to K_s. The coupling term for a given k_n value

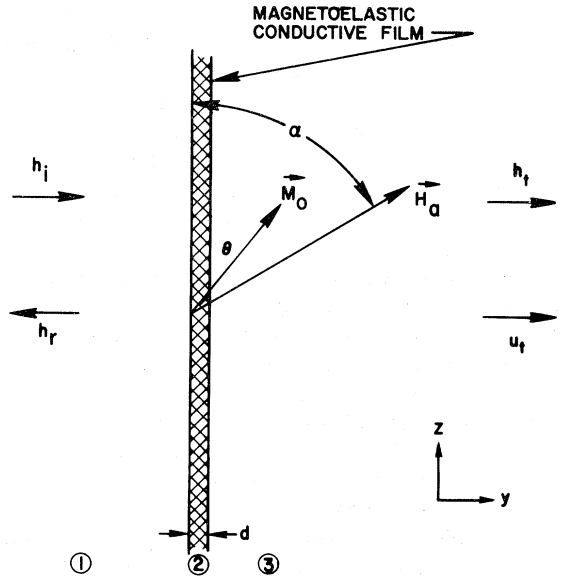

FIG. 1. Configuration of the film with respect to the static magnetic field and the em fields. Arrows associated with the field point along the propagation direction of the fields.

is of the order of

$$K_s' \cong \frac{k_n (B_2/M_0)^2}{\rho\omega^2 - C_{44} k_n^2}.$$

Assuming typical values of $B_2 \sim 10^7$ ergs/cm^3, $M_0 \sim 500$ G, $\rho \sim 9$ g/cm^3, $C_{44} \sim = 10^{12}$ dyn/cm^2, $\omega = 2\pi \times 10^{10}$ Hz, and $k_n \sim 10^4$ cm^{-1}, we obtain

$$K_s' \cong 10^{-10} \text{ erg/cm}^2.$$

K_s' is very small compared to typical values of the magnetic surface anisotropy constant, $\sim 10^{-1}$ erg/cm^2. However, K_s' may be important at the crossover region, since the expression in the denominator can become small. The denominator cannot become zero since k_n is complex. For oblique angles of $\vec{H}_a$ the boundary conditions on $\vec{m}$ based on uniaxial surface anisotropy are angle dependent.[10] The coupling term then depends both on B_1 and B_2. Nevertheless, K_s' arising from the coupling terms can be neglected for all angles of $\vec{H}_a$.

The boundary conditions on $\vec{u}$ for $\vec{H}_a$ normal to the film are given as

$$C_{44}\frac{\partial u}{\partial y} + \frac{B_2}{M_0} m + Z_A \dot{u} = 0, \quad y = d$$

$$C_{44}\frac{\partial u}{\partial y} + \frac{B_2}{M_0} m = 0, \quad y = 0.$$

If one assumes no coupling to the spin motion and a free surface, there would be no physical constraints on the lattice motion. This condition is

often referred to as the traction-free boundary condition. Since the films are magnetic and are usually prepared on substrates, one must introduce a physical constrain on the lattice motion by introducing the coupling term and the substrate acoustic impedance Z_A. For oblique angles of $\vec{H}_a$ the coupling term would be angle dependent and also depend on B_1. We will consider below the boundary conditions for $\vec{H}_a$ normal to the film. (When we consider the phenomena of transmission resonance at oblique angles, we will assume $B_1 = B_2 = 0$.) In the boundary conditions for u, the coupling term predominates.

(iv) The boundary conditions are written in terms of $h_n^{\pm}$ and applied surface field quantities so that unknown rf field variables can be found in terms of the incident field amplitude h_i.

III. MAGNETOACOUSTIC BOUNDARY CONDITIONS

In writing the magnetoacoustic boundary conditions for $\vec{H}_a$ normal to the film only three branches are magnetoacoustically active,[1] while four are not. For example, two of the branches are "magnetic" but are associated with circularly polarized waves in the opposite sense as the other two resonant magnetic branches.[1] One of the three elastic branches corresponds to the longitudinal-acoustic branch. This branch, as one of the transverse-acoustic branches, does not couple to the magnetic rf field.[1] The branches of interest are k_2, k_3, and k_7 as labeled in Ref. 1 (Figs. 5 and 6). Thus, we write

$$\sum_n (h_n^+ + h_n^-) = h_i + h_r, \quad y = 0 \tag{6}$$

$$\sum_n (h_n^+ e_+ + h_n^- e_-) = h_t e_0, \quad y = d \tag{7}$$

$$\frac{jc}{4\pi\sigma} \sum_n k_n (h_n^+ - h_n^-) = h_i - h_r, \quad y = 0 \tag{8}$$

$$\frac{jc}{4\pi\sigma} \sum_n k_n (h_n^+ e_+ - h_n^- e_-) = h_t e_0, \quad y = d \tag{9}$$

$$\sum_n Q_n (h_n^+ v_c + h_n^- v_d) = 0, \quad y = 0 \tag{10}$$

$$\sum_n Q_n (h_n^+ v_a e_+ + h_n^- v_b e_-) = 0, \quad y = d \tag{11}$$

$$\sum_n Q_n v_0 (h_n^+ + h_n^-) = 0, \quad y = 0 \tag{12}$$

$$\sum_n Q_n [h_n^+ (v_0 - v_n) e_+ + h_n^- (v_0 + v_n) e_-] = 0, \quad y = d. \tag{13}$$

Equations (6)–(9) represent the usual em boundary conditions. Equations (10) and (11) represent the dynamic pinning conditions on the rf magnetic moment. Equations (12) and (13) represent boundary conditions on $\vec{u}$. In these equations we have

$$\begin{aligned}
&Q_n = (1 - \tfrac{1}{2} j \delta^2 k_n^2)/4\pi, \quad \delta^2 = c^2/2\pi\sigma\omega, \\
&e_0 = e^{-jk_0 d}, \quad e_+ = e^{-jk_n d}, \quad e_- = e^{jk_n d}, \\
&k_0 = \omega/c, \quad k_n = k_2, k_3, \text{ and } k_7 \text{ (see Ref. 1)}, \\
&v_a = K_s^{(d)} - jk_n A, \quad v_b = K_s^{(d)} + jk_n A, \\
&v_c = K_s^{(0)} + jk_n A, \quad v_d = K_s^{(0)} - jk_n A, \\
&v_0 = B_2 [1 + C_{44} k_n^2/(\rho\omega^2 - C_{44} k_n^2)]/M_0, \\
&v_n = B_2 [Z_A \omega k_n/(\rho\omega^2 - C_{44} k_n^2)]/M_0.
\end{aligned} \tag{14}$$

In deriving v_a, v_b, v_c, and v_d we have neglected the coupling terms in the boundary conditions, for reasons mentioned above. However, the coefficients v_0 and v_n require the coupling terms. The relationship between the lattice displacement amplitudes $u_n^{\pm}$ and magnetic field amplitudes $h_n^{\pm}$ is given as[1]

$$u_n^{\pm} = \mp j (Q_n v_n / Z_A \omega) h_n^{\pm}, \tag{15}$$

where the superscript $\pm$ denotes waves traveling in the $\pm y$ direction. There are eight unknowns ($h_n^{\pm}$, h_r, and h_t) and eight equations, where $n = 2, 3$, and 7, h_r is the reflected field amplitude at the surface, and h_t is the transmitted field. The eight equations are solved numerically in terms of h_i, the incident field amplitude.

The transducer efficiency T is defined as

$$T = P_A / P_{\text{INC}},$$

where

$$P_A = \tfrac{1}{2} Z_A \omega^2 |u|^2,$$

$$u = \frac{1}{j\omega Z_A} \sum_n Q_n v_n (h_n^+ e_+ - h_n^- e_-),$$

and

$$P_{\text{INC}} = (c/8\pi) |h_i|^2.$$

The calculated transducer efficiency T is plotted in Fig. 2 as a function of (frequency field) ω/γ for a fixed external field of 9200 Oe. The characteristic parameters are appropriate to that of Ni: $4\pi M_0 = 6080$ G, $\gamma = 3.073 \times 10^6$ Hz/Oe, $\lambda = 3.75 \times 10^7$ Hz, $A = 0.9 \times 10^{-6}$ erg/cm, $2K_1/M_0 = -220$ Oe, $K_2 = 0$, $C_{44} = 1.22 \times 10^{12}$ dyn/cm^2, $C_{11} = 2.46 \times 10^{12}$ dyn/cm^2, $B_1 = 7.63 \times 10^7$ erg/cm^3, $B_2 = 8.54 \times 10^7$ erg/cm^3, $\sigma = 1.42 \times 10^5$ mhos/cm, and $\tau = 10^{-10}$ sec. We further assume that $K_s^{(d)} = K_s^{(0)} = 0$ so that there are no physical constraints on the motion of the magnetic moment at the two surfaces. It is noted in Fig. 2 that (i) maximum efficiency $T_{\max}$ occurs at magnetic resonance, which corresponds to a frequency

of ~9 GHz. T_{max} decreases with increasing thicknesses. The attenuation dependence of T_{max} on thickness is not a simple function of σ or τ. (ii) The transducer efficiency at the crossover frequency is lower than at resonance for the values of the parameters we have chosen. The resolution of the secondary peak in T improves with increasing thickness.

One interesting question is whether the subsidiary peak in efficiency observed by Bömmel and Dransfeld[13] at low fields may be due to some magnetoelastic coupling at the crossover region. It should be noted that if the frequency is fixed, as in the Bömmel and Dransfeld[13] experiment, and the field is varied, the secondary peak occurs at fields below ferromagnetic resonance. In Fig. 2 the field difference between the two peaks in T is about 200 Oe. At 1 GHz this difference should be smaller. Although it appears doubtful that our simple model can explain the subsidiary peak[13] at low fields, we have considered modifications of our model to explain Bömmel and Dransfeld's measurements.

In Fig. 3, the efficiency is plotted as a function of the applied field H_a at a fixed frequency of 1 GHz. We point out that the calculations use single-crystal parameters, whereas the experimental data of Bömmel and Dransfeld[13] were obtained from a polycrystalline film. However, we would expect only a few parameters to be different from the single-crystal parameters, and they are B_1, B_2, K_1, K_2, C_{11}, C_{44}, and σ. It may be possible to relate[16,17] B_1 and B_2 to magnetoelastic constants appropriate to a polycrystalline material. The effect of changing B_1 and B_2 is to change the conversion efficiency but not to change the field positions of T_{max} appreciably. The effect of changing the shear modulus is to change the crossover frequency, which means a shift in field position of the subsidiary peak but *not* a shift in the main peak. Generally, the value of σ is lower in a polycrystalline film than it is in a bulk single crystal. Magnetocrystalline anisotropy effects will not shift the line appreciably but may cause some broadening in a polycrystalline material. Finally, the value of A as chosen by us may not be appropriate for the films used in the experiment. However, we expect a reasonable value of A to be within 20% of our assumed value.

We have also considered the effects of variation of C_{44} on the field position of the subsidiary peak. For example, for $C_{44} = 1.22 \times 10^{12}$ dyn/cm^2, the two peaks are nearly overlapping. By lowering C_{44} to 0.85×10^{12} dyn/cm^2 and lowering the elastic damping by the same percentage amount, we obtain a similar separation as before of 100 Oe between the two peaks but with improved definition. This is compared to a separation of 1000 Oe as observed by Bömmel and Dransfeld.[13] Obviously, it will require an unreasonable amount of change in C_{44} and A to obtain a separation of 1000 Oe. Spin-wave standing mode resonance coupled to the elastic motion can be dismissed as a mechanism to explain the low-field peak, since the film is too thick (1.8 μm) to support standing spin waves. Because of the low field at which this peak is located, the sample cannot be magnetically saturated and we surmise that the absorption is associated with some magnetic domain resonance. Our cal-

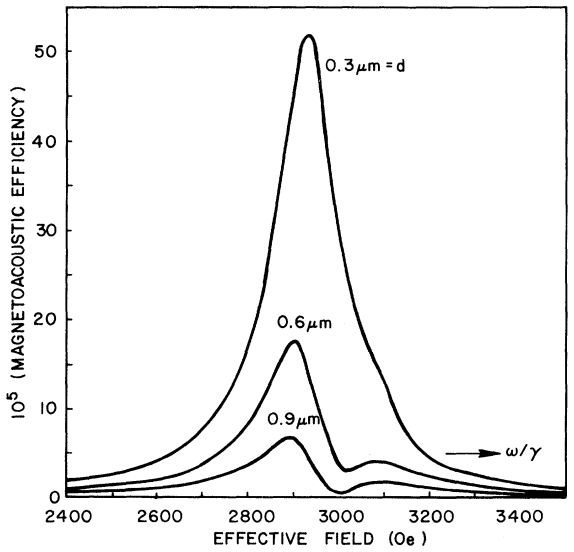

FIG. 2. Magnetoacoustic efficiency as a function of "effective field" for Ni films of different thicknesses. A constant bias field of 9200 Oe is applied perpendicular to the film plane. Parameters are given in the text.

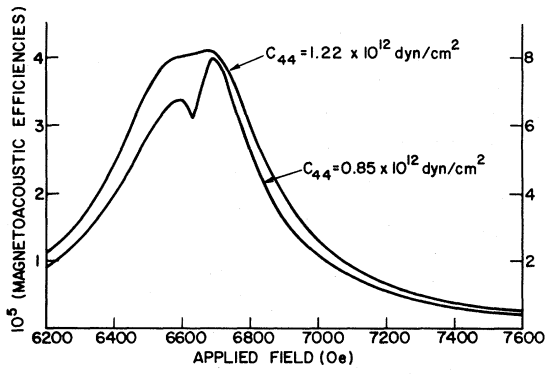

FIG. 3. Magnetoacoustic efficiency as a function of applied field for a 1.8-μm-thick Ni film. A constant frequency of 1 GHz is applied. Upper curve is the result of calculations using the same parameters as Fig. 2. Lower curve shows the effect of choosing a smaller value for C_{44} (see scale on the right-hand side).

culations are not sufficiently general to quantitatively calculate this effect.

In our calculations it is assumed that the film is *uniformly* magnetized for fields below $4\pi M_0$. Thus, our calculations are applicable for $H_a \geq 4\pi M_0$. Conceivably, one could apply the calculations in the regime of $H_a < 4\pi M_0$ provided the average magnetization is known *a priori* as a function of the applied field H_a.

It is not necessary to do a full calculation of the line shape to arrive at our conclusions in regard to the subsidiary peak at low fields. However, if quantitative values for efficiency, bandwidth, and practical limits for transducer applications are required, one needs to use the full "apparatus" of the calculation.

As another example, the Tb-Fe rare-earth transition system is often quoted as a plausible system for transducer application at microwave frequencies, since the magnetostriction is large in this system. Donoho[14] *et al.* fabricated and tested a transducer of Tb-Fe film and found reasonable efficiencies at room temperature and at a frequency of ~1 GHz. We have calculated the line shape assuming parameters appropriate to Tb-Fe: $C_{44} = 10^{12}$ dyn/cm^2, $K_1 = K_2 = 0$, $\lambda = 3.75 \times 10^7$ Hz, $\sigma = 0.7 \times 10^5$ mhos/cm, $4\pi M_0 = 6100$ G, $B_2 = -10^9$ erg/cm^3. In assigning a value for B_2 we have assumed a conservative (lower) value, since (i) it is not clear from previous work[14] whether the film was polycrystalline or amorphous, and (ii) the film composition is not known. In Fig. 4 it is seen that the calculated maximum efficiency occurs below magnetic resonance and at the crossover field. This may result from our choice of magnetic and elastic damping rather than being intrinsic to Tb-Fe. Nevertheless, we see that even assuming conservative values for B_2, good transducer efficiencies can be realized in this system. The experimental data is that of Donoho *et al.*[14] Better agreement with this data may be possible through use of a much larger relaxation parameter λ. However, because the cause of the experimental linewidth in Fig. 4 is not known, and may more realistically be related to a distribution of magnetic anisotropy or magnetostrictive fields, we have not gone further in attempting to fit the line shape without a more detailed knowledge of the magnetic properties of the Tb-Fe films.

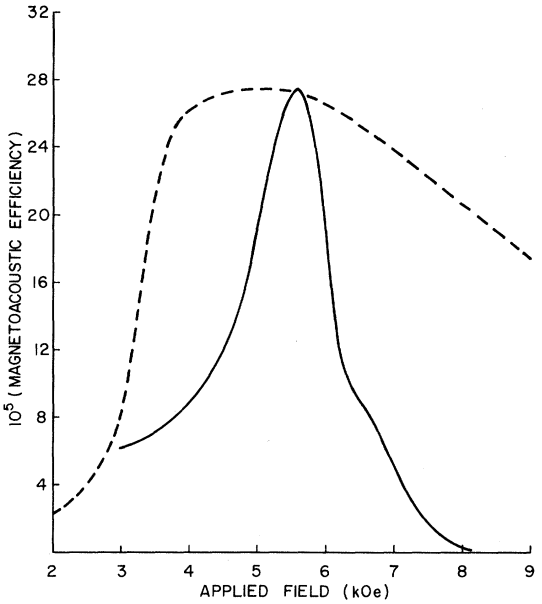

FIG. 4. Magnetoacoustic efficiency as a function of applied field for a 1.8-μm-thick film with parameters chosen to approximate $TbFe_2$ (solid curve). Applied frequency for the calculation is 1 GHz. Experimental data (dashed curve) was obtained from Fig. 2, of Ref. 14 (the applied frequency is 0.69 GHz). Because no absolute numbers are given for the efficiencies in Ref. 14, experimental data have been normalized such that the theoretical and experimental maxima are equal.

IV. FERROMAGNETIC TRANSMISSION RESONANCE

For this part of the calculation we put $B_1 = B_2 = 0$ so that we are considering "pure" electromagnetic effects. Acoustic effects on transmission resonance can be simply considered by making use of the full set of boundary conditions. By neglecting acoustic effects the number of equations in the boundary conditions reduce, since $\vec{u} = 0$. Let us now consider the boundary conditions for transmission resonance for all angles of H_a instead of only normal to the film:

$$\sum_n (h_n^+ + h_n^-) = h_{ix} + h_{rx}, \qquad y = 0 \qquad (16)$$

$$\sum_n (h_n^+ + h_n^-) p_n = h_{iz} + h_{rz}, \qquad y = 0 \qquad (17)$$

$$\sum_n (h_n^+ e_+ + h_n^- e_-) = h_{tx} e_0, \qquad y = d \qquad (18)$$

$$\sum_n (h_n^+ e_+ + h_n^- e_-) p_n = h_{tz} e_0, \qquad y = d \qquad (19)$$

$$\frac{jc}{4\pi\sigma} \sum_n k_n (h_n^+ - h_n^-) = h_{ix} - h_{rx}, \qquad y = 0 \qquad (20)$$

$$\frac{jc}{4\pi\sigma} \sum_n k_n p_n (h_n^+ - h_n^-) = h_{iz} - h_{rz}, \qquad y = 0 \qquad (21)$$

$$\frac{jc}{4\pi\sigma} \sum_n k_n (h_n^+ e_+ - h_n^- e_-) = h_{tx} e_0, \qquad y = d \qquad (22)$$

$$\frac{jc}{4\pi\sigma} \sum_n k_n p_n (h_n^+ e_+ - h_n^- e_-) = h_{tz} e_0, \qquad y = d \qquad (23)$$

$$\sum_n Q_n[h_n^+(K_s^{(0)}\cos 2\theta - jk_nA) + h_n^-(K_s^{(0)}\cos 2\theta + jk_nA)] = 0, \quad y=0 \tag{24}$$

$$\sum_n Q_n p_n[h_n^+(K_s^{(0)}\sin^2\theta + jk_nA) + h_n^-(K_s^{(0)}\sin^2\theta - jk_nA)] = 0, \quad y=0 \tag{25}$$

$$\sum_n Q_n[h_n^+ e_+(K_s^{(d)}\cos 2\theta + jk_nA) + h_n^- e_-(K_s^{(d)}\cos 2\theta - jk_nA)] = 0, \quad y=d \tag{26}$$

$$\sum_n Q_n p_n[h_n^+ e_+(K_s^{(d)}\sin^2\theta - jk_nA) + h_n^- e_-(K_s^{(d)}\sin^2\theta + jk_nA)] = 0, \quad y=d. \tag{27}$$

The first eight equations require that both the x and z components of the magnetic and electric fields be continuous at the two surfaces. For oblique angles of $\vec{H}_a$ all four[1] magnetic branches of k_n are required. The dependence of k_n on ω and H_a are calculated in Ref. 1. For each k_n value the relationship between the z and x components of $h_n^\pm$ is given as[18]

$$p_n = \frac{(h_n^\pm)_z}{(h_n^\pm)_x} = \frac{b_n \sin\theta}{d_n\cos^2\theta + a_n\sin^2\theta + \Omega},$$

where

$$b_n = H_0 + M_0/Q_n + 2Ak_n^2/M_0,$$

$$a_n = \lambda[(H_0 + 2Ak_n^2/M_0)/M_0 + 1/Q_n]/\gamma,$$

$$d_n = \lambda[(H_0 + 2Ak_n^2/M_0)/M_0 + 4\pi]/\gamma.$$

[In the equations of this section we abbreviated $(h_n^\pm)_x$ as $h_n^\pm$.] We will assume that the incident wave is linearly polarized along the x direction so that $h_{tx}=1$ and $h_{tz}=0$. Although $h_{tz}=0$, the transmitted and reflected waves, h_t and h_r, will contain a component along the z direction, since they are elliptically polarized for oblique angles and circularly polarized for $\vec{H}_a$ normal to the film. For $\vec{H}_a$ in the plane, there is *no* reflected and transmitted wave component along the z direction. Finally, the last four equations represent the pinning conditions on $\vec{m}$ and they are[10]

$$A\frac{\partial m_z}{\partial n} + m_z K_s \sin^2\theta = 0,$$

$$A\frac{\partial m_x}{\partial n} - m_x K_s \cos 2\theta = 0.$$

The surface anisotropy constant K_s may be chosen to be different at the two surfaces. We have assumed that the orientation of the static magnetization is the same throughout the sample, although this assumption may not be valid if K_s is large. Obviously, this pinning condition is angle dependent, and the angle θ of the magnetization with respect to the film plane follows from the equilibrium condition,

$$H_a\sin(\alpha-\theta) = 2\pi M_0 \sin 2\theta. \tag{28}$$

The internal field H_0 is defined in terms of the applied field as

$$H_0^2 = H_a^2\cos^2\alpha + (H_a\sin\alpha - 4\pi M_0\sin\theta)^2. \tag{29}$$

For fixed oblique angles α, the angle θ varies continuously as the magnitude of H_a is swept. This presents a situation in which the pinning conditions change as H_a is swept. We have taken this into account in our solutions. This problem does not arise for the in-plane and perpendicular cases, for which the static magnetization remains fixed in orientation. Finally, the transmitted rf magnetic fields h_{tx} and h_{tz} are calculated in terms of h_{ix} using the 12 equations above, as a function of H_a at fixed frequency.

We find from our numerical solutions that the field position and line shapes for $\alpha=0$ and 90° are in essential agreement with those discussed in Ref. 8 (see Fig. 5). In Fig. 6 we show the results of our detailed calculations for the position and width (at $\frac{1}{2}$ of the maximum of h_{tx}) using the parameters reported by Heinrich and Cochran.[8] In our calculation, the width is seen to increase rapidly as $90°-\alpha$ increases as a result of the "mechanical" rotation of $\vec{M}_0$. This rapid rotation is a consequence of having H_a only slightly above $4\pi M_0$ and makes the angular alignment of H_a very critical in the experimental arrangement. Use of higher frequencies would considerably reduce such broadening. In our calculations, all of the exchange modes are included and the pinning conditions are found to be unimportant for thick films. Using the parameters quoted in Fig. 6, variation of K_s from 0 to ∞ (including 1, 10, and 1000 erg/cm²) pro-

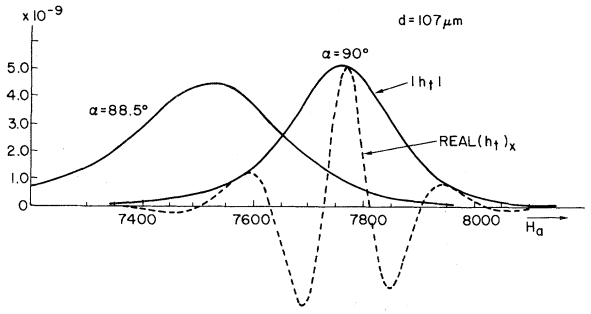

FIG. 5. Transmitted field amplitudes as a function of applied field for a 107-μm-thick $Ni_{0.90}$ and $Fe_{0.10}$ film at a frequency of 23.7 GHz. Constant field is applied at 90° and 88.5° out of the film plane. Parameters used are $\omega/\gamma = 7770$ Oe, $4\pi M_0 = 6950$ G, $d/\delta = 60$, $A = 10^{-6}$ erg/cm, and $\lambda = 0.27\times 10^7$ Hz.

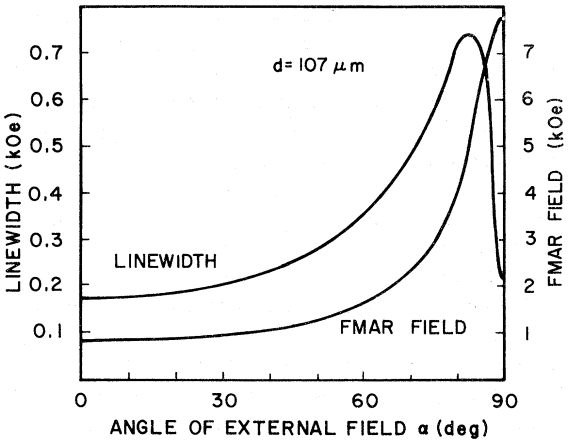

FIG. 6. Linewidth and field for maximum transmission as a function of the angle of the applied field from the film plane for the Ni-Fe film of Fig. 5. Parameters are those given by Heinrich and Cochran (Ref. 8).

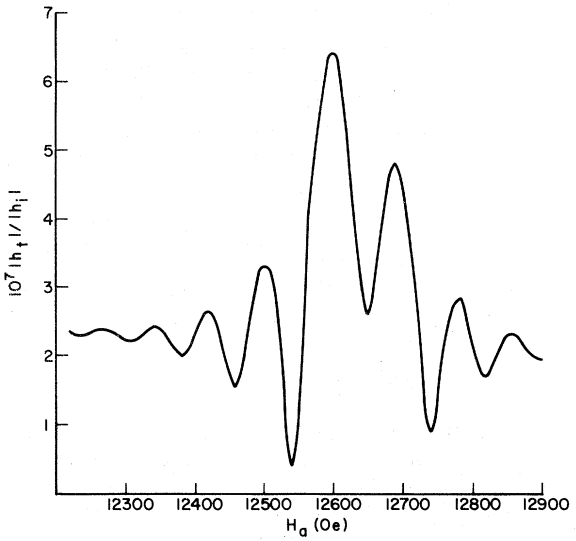

FIG. 7. Transmitted field amplitude as a function of applied field for a 10-μm film of permalloy at 4.2 K. Parameters are those given by Phillips (Ref. 6).

duces only about 0.001% changes in transmitted intensity. However, in thin films on the order of 10 μm, we find a number of transmission maxima (Fig. 7) corresponding to standing modes of long wavelength. This contrasts to the results of Fig. 1 of Ref. 6, where only two peaks are shown. In fact, using Eq. (7) of Ref. 6 for the transmittance with the same parameters given in this reference we still find a number of transmission peaks instead of only two.

V. APPROXIMATE CALCULATIONS FOR TRANSMISSION RESONANCE

As pointed out previously,[3] when the classical skin depth δ is on the order of the film thickness, the transmission becomes very flat near ferromagnetic antiresonance (FMAR) except that the dimensional spin-wave resonances can be seen in transmission. In this regime the results are quite sensitive to surface pinning, but the FMAR is poorly defined. The regime studied in most transmission experiments is $\delta \ll d$. Under these conditions, the FMAR becomes progressively sharper and the effects of surface pinning are negligible. The waves with large wave vectors k are weighted correspondingly less so that only the longest-wavelength solution of the secular equation is important for FMAR in thick films. The approximate value of k near FMAR is given by $k = (1/\delta)(\Delta H/2\pi M_0)^{1/2}$, where $\Delta H = 2(\lambda/\gamma)(\omega/\gamma M_0)$ is the FMR half-power linewidth neglecting exchange effects and λ is the Landau-Lifshitz damping parameter. This thickness regime can be further divided into $\delta < d < \delta(2\pi M_0/\Delta H)^{1/2}$ and $\delta(2\pi M_0/\Delta H)^{1/2} < d$. In the former case the film is still largely transparent at the antiresonance, and in the latter, the waves at antiresonance are strongly attenuated in a single passage, but may still be easily observable. In the latter case, the transmitted-wave amplitude is given essentially by e^{-kd}, where k is the wave vector evaluated at antiresonance.

We have retained the exact low-order terms in k from the secular equation,[1] and have analyzed the field dependence of k near its minimum in order to determine the transmission line shape. In particular, we make the approximation of neglecting terms of order k^4 and higher compared to k^2 and neglecting reflected waves. The first approximation is equivalent to neglecting exchange fields, $2Ak^2/M_0$, which are very small near the FMAR. We then consider the line shape to be determined by $e^{-dk(H_0)}$ in order to generate a useful approximation.

We observe first that for oblique angles, the propagation constant at the transmission maximum is given by (see Ref. 19)

$$k \simeq [\lambda\omega(1 - \sin^2\theta)/\pi\gamma^2 M_0^2]^{1/2}/\delta . \tag{30}$$

Thereby, the transmission efficiencies at FMAR are angle dependent, reaching a minumum for $\alpha = \theta = 0$. The FMAR linewidth can be determined from the field dependence of k near the transmission maximum. Kaganov[19] has adapted a similar approach. However, his approximations omit the damping terms and are therefore not appropriate for most of the experiments on thick films except far from the FMAR. For thick films, i.e., roughly for $d > \delta(2\pi M_0/\Delta H)^{1/2}$, the transmission line shape

is nearly Gaussian, because $k(H_0)$ is in the neighborhood of a minimum, with the predominant field dependence being $k \propto H_0^2$. However, the odd powers of H_0 also appear weakly if k is expanded in powers of H_0 and they produce a small shift and skewing of the line shape. The linewidth, which we define as the separation of the applied dc fields required to reduce the transmitted field amplitudes by $\frac{1}{2}$ from the maximum, is found to be approximately

$$\Delta H_{\mathrm{FMAR}} \simeq 1.2\pi M_0[(\delta_0/d)(\Delta H/M_0)^{3/2}]^{1/2}, \qquad (31)$$

where

$$\delta_0^2 = \delta^2(1+\sin^2\theta).$$

We compared the approximate ΔH_{FMAR} expression for $\theta = 0$ and 90° against our exact solution and we find it to be accurate to 10%. The transmission resonance condition is now approximated to be

$$\omega/\gamma \cong B_0 + 2\Delta H^2/[4\pi M_0(1+\sin^2\theta)].$$

The first term represents the antiresonance condition for an insulator with no magnetic losses. By including losses a small but measurable field shift is introduced in the antiresonance condition. Equation (31) is independent of the form of damping assumed. The field width is given in terms of the internal field of Eq. (29); it is equal to the external field width only for $\alpha = 0$ or 90°. However, using Eqs. (28) and (29), the width can be approximately corrected for the effects of rotation of the magnetization.

VI. DISCUSSIONS AND CONCLUSIONS

The calculations contain various degrees of freedom in the equations of motion and at the surfaces so that one can calculate a number of phenomena. In this paper the electromagnetic and magnetoacoustic transmission in metal films is calculated. Ferromagnetic resonance in metal films has been discussed extensively in the literature and there is no need to calculate this effect here. Besides the aforementioned effects, it may be possible to observe the effect of magnetoacoustic interaction on FMAR, since both the FMAR field and the spin waves and elastic branches are degenerate for fields below FMR. This should be an interesting effect to observe and calculate from our formulation.

For our two example calculations we conclude that:

(i) Although we assumed a conservative value for the magnetoelastic parameter and conductivity for $TbFe_2$, practical (~30 dB) transducer efficiency is realized at microwave frequencies and for a thickness of ~2 μm. In most materials maximum transducer efficiency has been observed at FMR. If the elastic damping is assumed in the calculation to be unusually small, maximum efficiency would occur at the crossover region.

In recent[20] experiments magnetoacoustic conversion has been observed in $TbFe_2$ polycrystalline films as thick as ~3–4 μm. Maximum conversion efficiency occurred for a thickness of ~1.1 μm. This thickness corresponds to one-half of the acoustic transverse wavelength and standing acoustic modes are excited in this case. It may be possible to enhance the magnetoacoustic conversion by purposely choosing the film and substrate acoustic impedances to be very different.

(ii) Our exact calculations of the FMAR transmission efficiencies are in good agreement with the work of Cochran *et al.*[9] The approximate expression for the FMAR field and linewidth should be very useful for studying directly the intrinsic damping in thick films. For thinner films there is *considerable* structure in transmission, making them potentially promising for experimental and theoretical studies.

[1] C. Vittoria, N. J. Craig, and G. C. Bailey, Phys. Rev. B 10, 3945 (1974).
[2] M. I. Kaganov, Fiz. Met. Metalloved. 7, 288 (1959).
[3] B. Heinrich and V. G. Meshcheryakov, Zh. Eksp. Teor. Fiz. Pis'ma Red. 9, 618 (1969) [JETP Lett. 9, 378 (1969)].
[4] C. Kittel, J. Phys. Radium 12, 291 (1951).
[5] W. S. Ament and G. T. Rado, Phys. Rev. 97, 1558 (1955).
[6] T. G. Phillips, J. Appl. Phys. 41, 1109 (1970).
[7] O. Horan *et al.*, Phys. Rev. Lett. 25, 246 (1970).
[8] B. Heinrich and J. F. Cochran, Phys. Rev. Lett. 29, 1175 (1972).
[9] J. F. Cochran and B. Heinrich, and G. Dewar, AIP Conf. Proc. 24, 509 (1974).
[10] P. Lubitz and C. Vittoria, AIP Conf. Proc. 24, 507 (1974).
[11] C. Kittel, Phys. Rev. 110, 836 (1958).
[12] T. Kobayashi, R. C. Barker, and A. Yelon, IEEE Trans. Magn. 7, 755 (1971).
[13] H. Bömmel and K. Dransfeld, Phys. Rev. Lett. 3, 83 (1972).
[14] P. L. Donoho *et al.*, AIP Conf. Proc. 10, 769 (1972).
[15] V. A. Ignatchenko and E. V. Kuz'min, Fiz. Tverd. Tela 7, 1962 (1965) [Sov. Phys.-Solid State 7, 1585 (1966)].
[16] E. Callen, J. Appl. Phys. 36, 976 (1965).

[17]E. V. Vladimizsky, C. R. (Dokl.) Acad. Sci. URSS 41, 10 (1943).
[18]C. Vittoria, R. C. Barker, and A. Yelon, J. Appl. Phys. 40, 1561 (1969).
[19]M. I. Kaganov, Zh. Eksp. Teor. Fiz. Pis'ma Red. 10, 336 (1969) [JETP Lett. 9, 378 (1969)].
[20]L. B. McLane, P. L. Donoho, and W. L. Wimbush, AIP Conf. Proc. 24, 653 (1974).